Acta Crystallographica Section B
Structural Science
ISSN 0108-7681

Synthesis, structure, thermal and non-linear optical properties of L-argininium hydrogen selenite

E. de Matos Gomes,[a]* E. Nogueira,[a] I. Fernandes,[a] M. Belsley,[a] J. A. Paixão,[b] A. Matos Beja,[b] M. Ramos Silva,[b] J. Martín-Gil,[c] F. Martín-Gil[c] and J. F. Mano[d]

[a]Departamento de Física, Universidade do Minho, Largo do Paço, P-4719 Braga Codex, Portugal, [b]CEMDRX, Departamento de Física, Universidade de Coimbra, P-3004-516 Coimbra, Portugal, [c]Departamento de Química Inorganica, Paseo del Cauce, SP-47011, Valladolid, Spain, and [d]Departamento de Engenharia de Polímeros, Universidade do Minho, Campus de Azurém, P-4800-058 Guimarães, Portugal

Correspondence e-mail: emg@fisica.uminho.pt

L-Argininium hydrogen selenite ($C_6H_{15}N_4O_2HSeO_3$) is a new semiorganic compound of the hydrogen selenite family with non-linear optical properties. The crystal lattice is monoclinic with unit-cell parameters a = 22.493 (5), b = 5.1624 (13), c = 9.730 (4) Å, β = 95.68 (3)°, V = 1124.3 (6) Å^3, Z = 4, space group $C2$. Second-harmonic generation measurements performed on powder samples, using a Q-switched Nd:Yag laser (λ = 1064 nm), showed the second-harmonic power to be about twice that of urea. Differential scanning calorimetry measurements revealed the existence of a phase transition with onset at 289 K.

Received 24 May 2001
Accepted 14 June 2001

Supplementary data for this paper are available from the IUCr electronic archives (Reference: NA0124). Services for accessing these data are described at the back of the journal.

1. Introduction

L-Arginine is an amino acid that occurs widely in biological substances. Owing to the strong basicity of the guanidyl group, it easily forms salts with acids such as phosphoric, fluoridric and chloridric acids (Monaco *et al.*, 1987).

L-Arginine phosphate monohydrate, known as LAP (Aoki *et al.*, 1971), and in particular its deuterated form are efficient crystals for frequency conversion owing to their non-linear optical properties. LAP is phase matchable with all non-linear processes, whereas potassium dihydrogen phosphate (KDP) is phase matchable (Eimerl *et al.*, 1989). LAP is three times more linear than KDP, its damage threshold is about three times higher than KDP and it is also more angularly sensitive (Monaco *et al.*, 1987; Yokotani *et al.*, 1989).

With the aim of extending the number of LAP analogs with potential applications in non-linear optics, we have attempted the synthesis of L-arginine with selenious acid and a new material with non-linear optical properties, L-argininium hydrogenselenite hydrate, was obtained.

2. Experimental

2.1. Synthesis and thermal behavior

L-Argininium·$HSeO_3$ (hereafter LAHSe) is obtained by mixing an aqueous solution of L-arginine and selenious acid in a 1:2 molar ratio. After stirring for ~1 h above room temperature, the solution was allowed to cool down to room temperature and kept at 243 K for several weeks, after which very small crystals formed in a gel solution. The crystals obtained have a very small size, < 0.5 mm.

Differential scanning calorimetry to characterize the thermal behavior of LAHSe was performed using a Perkin-Elmer DSC7 apparatus. The sample, weighing 14.980 mg, was measured from 253 to 423 K at a rate of 10 K min^{-1}. The DSC trace is shown in Fig. 1. One detects two transitions. At lower temperature there is a second-order-like phase transition at 289 K (temperature of inflexion of the curve) and an increase of the heat capacity of $\Delta C_p = 0.21$ J Kg^{-1}. The peak which appears at higher temperatures corresponds to a first-order transition, probably assigned to the melting point of the material. However, the drastic decrease of the signal after the maximum which drifts well below the initial base line suggests a degradation process of LAHSe in the same temperature range of the endothermic process.

2.2. Linear and non-linear optical properties

Owing to the difficulty of growing crystals with a size suitable for linear transmission measurements, the transmission curve of an aqueous solution of LASe (0.1 *M*) was measured at room temperature. As shown in Fig. 2, it has a transmission above 80% from 400 to 1100 nm. Second-harmonic generation (SHG) measurements, relative to urea, were performed on polycrystalline samples, using the powder technique known as the Kurtz test (Kurtz & Perry, 1968). The fundamental beam of a *Q*-switched Nd:Yag laser with a 1064 nm nanometer wavelength, pulse duration of 7 ns and a 10 Hz repetition rate was weakly focused on the samples. The second harmonic signal was separated from the incident fundamental beam using dichroic mirrors and then set into a monochromator. The signal was detected using a photomultiplier tube (type 1P28 at 900 V bias) and read using a fast digital oscilloscope (Tektronix TDS 520 with a bandwidth of 500 MHz). Averages over 100 laser shots were acquired in order to reduce the influence of shot-to-shot variations in laser power. A second harmonic power twice that of urea was measured.

2.3. Structure determination and refinement

Data collection was performed on a *CAD*-4 X-ray diffractometer using Mo $K\alpha$ radiation (λ = 0.71073 Å). Cell parameters were obtained from a least-squares fit of 25 reflections. A total of 5336 reflections (2674 unique) were measured at room temperature, in the range $3.6 \leq \theta \leq 30.0°$, of which 2542 unique reflections had $I > 2\sigma I$. Full profile ω–2θ scans were measured and analysed to extract the intensities. Three standard and three orientation control reflections were measured every 180 reflections. The crystal showed no appreciable decay during data collection. Data reduction was performed with *HELENA* (Spek, 1997). An absorption correction was applied to the data based on a set of nine Ψ scan curves (North *et al.*, 1968). The scaled maximum and minimum transmission factors were 0.432 and 0.251. After absorption correction the internal agreement factor between equivalent reflections was $R_{\rm int} = 1.87\%$, which compares well with the statistic accuracy of the data-set [average $\sigma_I/I_{\rm av} = 1.99\%$]. The structure was solved by direct methods using *SHELXS*97 (Sheldrick, 1997*b*) and refined with *SHELXL*97 (Sheldrick, 1997*a*). The calculations were performed on a Pentium 330 MHz PC running *LINUX*.

All H atoms were clearly seen on a difference-Fourier map, except those of a highly disordered solvent (water) molecule (see below). The coordinates of all H atoms were refined with an isotropic displacement parameter equal to $1.2U_{\rm eq}$ of the parent atom for NH_2, CH and CH_2 groups, or $1.5U_{\rm eq}$ of the parent atom for the NH_3 and OH groups, starting from calculated positions. Refinement of the Flack parameter [x = 0.013 (8)] confirmed that the absolute configuration was correctly chosen, which corresponds to the well known *S* configuration of the chiral C_α atom of L-arginine. Further details concerning the data collection and structure refinement are gathered in Table 1.

Examination of the crystal structure with *PLATON* (Spek, 2001) showed the presence of two voids in the crystal lattice of ~20 Å^3 each at the two equivalent positions 1/2, −0.122, 1/2; 0, 0.378, 1/2. As the residual density at these positions was

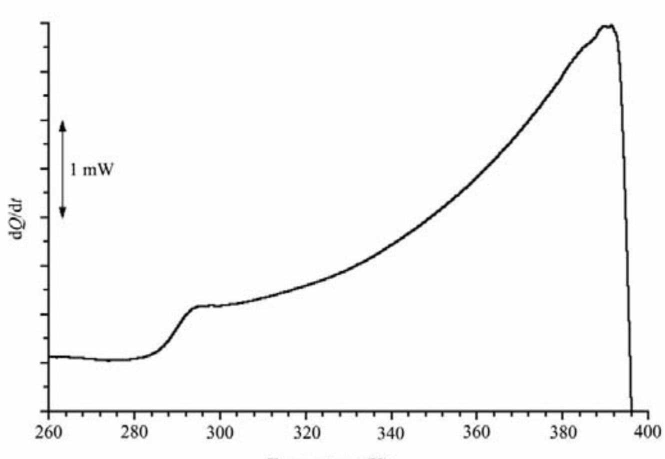

Figure 1
Differential scanning calorimetry of LAHSe, showing a phase transition at 289 K.

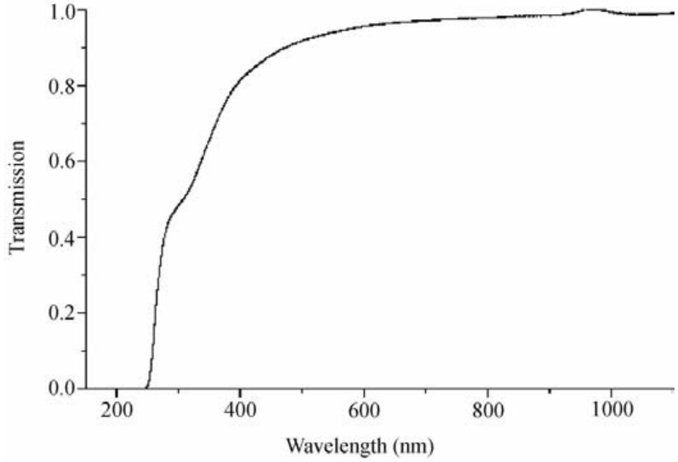

Figure 2
Transmission curve of an aqueous 0.1 *M* solution of LAHSe.

Table 1
Experimental details.

Crystal data	
Chemical formula	$C_6H_{15}N_4O_2^+\cdot HSeO_3^-\cdot 0.1525H_2O$
Chemical formula weight	305.93
Cell setting, space group	Monoclinic, C_2
a, b, c (Å)	22.493 (5), 5.1624 (13), 9.730 (4)
β (°)	95.68 (3)
V (Å^3)	1124.3 (6)
Z	4
D_x (Mg m^{-3})	1.807
Radiation type	Mo $K\alpha$
No. of reflections for cell parameters	25
θ range (°)	5.51–15.43
μ (mm^{-1})	3.357
Temperature (K)	293 (2)
Crystal form, color	Block, light red
Crystal size (mm)	0.38 × 0.35 × 0.25
Data collection	
Diffractometer	Enraf–Nonius CAD-4
Data collection method	Profile data from ω–2θ scans
Absorption correction	Psi-scan
$T_{\min}$	0.251
$T_{\max}$	0.432
No. of measured, independent and observed parameters	5336, 2674, 2542
Criterion for observed reflections	$I > 2\sigma(I)$
$R_{\rm int}$	0.0187
$\theta_{\max}$ (°)	29.98
Range of h, k, l	$-31 \rightarrow h \rightarrow 31$ $-6 \rightarrow k \rightarrow 7$ $-13 \rightarrow l \rightarrow 13$
No. and frequency of standard reflections	3 every 180 reflections
Intensity decay (%)	1.34
Refinement	
Refinement on	F^2
$R[F^2>2\sigma(F^2)]$, $wR(F^2)$, S	0.0223, 0.0598, 1.053
No. of reflections and parameters used in refinement	2674, 200
H-atom treatment	Mixed
Weighting scheme	$w = 1/[\sigma^2(F_o^2) + (0.0450P)^2 + 0.2447P]$, where $P = (F_o^2 + 2F_c^2)/3$
$(\Delta/\sigma)_{\max}$	0.001
$\Delta\rho_{\max}$, $\Delta\rho_{\min}$ (e Å^{-3})	0.331, −0.512
Extinction method	*SHELXL*97 (Sheldrick, 1997*b*)
Extinction coefficient	0.0046 (6)

Computer programs used: *CAD*-4 (Enraf–Nonius, 1989), *HELENA* (Spek, 1997), *SHELXS*97 (Sheldrick, 1997*a*), *SHELXL*97 (Sheldrick, 1997*b*).

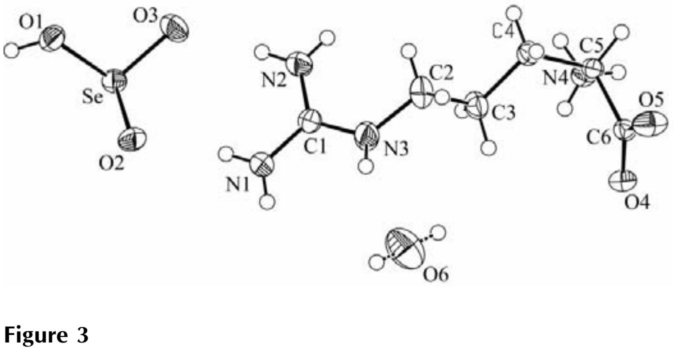

Figure 3
*ORTEP*II (Johnson, 1976) drawing of the title compound. Displacement ellipsoids are drawn at the 50% level.

Table 2
Selected geometric parameters (Å, °).

Se—O	1.649 (2)	N2—C1	1.319 (3)
Se—O2	1.659 (2)	N3—C1	1.326 (3)
Se—O1	1.791 (2)	O3—Se—O2	104.7 (1)
O4—C6	1.241 (3)	O3—Se—O1	99.6 (1)
O5—C6	1.251 (3)	O2—Se—O1	100.50 (9)
N1—C1	1.333 (3)		

relatively high (1.55 e Å^{-3}) we considered the possibility of occupation by a disordered water molecule, despite the small volume of the voids. Including such a disordered water molecule in the refinements dropped the R factor from 2.65 to 2.23% and the residual density showed no significant features. The final refined site occupancy of the water molecule was 30.5 (11)%; full occupancy of the site would correspond to a composition of half a molecule of water to each LASe formula unit. Therefore, the highly disordered water molecule corresponds to a very small degree of hydration of the LAHSe salt. It was not possible to locate on a difference-Fourier synthesis the H atoms of the solvent water molecule. Tentative coordinates for the water H atoms were obtained from a force-field calculation which performs an energy minimization of the van der Waals and Coulomb non-bonded energy profiles around a set of starting points that takes into account the neighboring hydrogen-bond acceptors and reasonable geometric criteria for hydrogen bonding (Nardelli, 1999). An O—H bond distance of 0.850 Å was assumed. The best coordinates for the water H atoms, corresponding to the minimum of the energy profile, were then included in the refinement riding on the O atom with an isotropic $1.5U_{\rm eq}$(O).

Fig. 3 depicts an *ORTEP*II (Johnson, 1976) plot of the structure. A selection of relevant bond distances and valence angles are given in Table 2.

3. Discussion

Inspection of the anion bond distances shows the presence of two short and one long Se—O bond, clearly indicating that one H atom is attached to the O1 atom and that both O2 and O3 atoms are bare. This observation, and the objective localization of the H atoms on a difference-Fourier map, confirms that one of the protons was transferred from the acid to the arginine molecule. The geometry of the anion is similar to that found in other hydrogenselenite salts (Matos Gomes *et al.*, 1995; Paixão *et al.*, 1997).

The cation exists as positively charged zwitterions, in which the guanidyl and amino groups are protonated and the carboxyl group is deprotonated, as shown by the C—O distances [C6—O4 1.241 (3), C6—O5 1.251 (3) Å; average C—O distance of a carboxylate group from the Cambridge Structural Database: 1.254 (10) Å (Allen *et al.*, 1987)]. The C_γ atom (C3) is in a staggered *gauche* position to both the amino and carboxyl groups. The torsion angles fully describing the conformation of the cation, as defined by the IUPAC-IUB Commission on Biochemical Nomenclature (1975) are: φ^1 = O4—C6—C5—N4 −19.1 (3), φ^2 = O5—C6—C5—N4

Table 3
Hydrogen-bonding geometry (Å, °).

$D-\mathrm{H}\cdots A$	$D-\mathrm{H}$	$\mathrm{H}\cdots A$	$D\cdots A$	$D-\mathrm{H}\cdots A$
$\mathrm{O1-H1\cdots O2^{i}}$	0.90 (4)	1.80 (4)	2.696 (3)	172 (3)
$\mathrm{N1-H1}A\cdots\mathrm{O2^{ii}}$	0.83 (3)	2.01 (3)	2.830 (3)	169 (3)
$\mathrm{N1-H1}B\cdots\mathrm{O5^{iii}}$	0.78 (3)	2.10 (3)	2.868 (3)	167 (3)
$\mathrm{N2-H2}A\cdots\mathrm{O3}$	0.83 (4)	2.06 (4)	2.887 (3)	174 (3)
$\mathrm{N2-H2}B\cdots\mathrm{O3^{ii}}$	0.86 (3)	2.02 (3)	2.879 (3)	176 (3)
$\mathrm{N3-H3\cdots O4^{iv}}$	0.82 (3)	2.08 (3)	2.890 (3)	168 (3)
$\mathrm{N4-H4}A\cdots\mathrm{O5^{v}}$	0.81 (3)	2.08 (3)	2.871 (3)	165 (3)
$\mathrm{N4-H4}B\cdots\mathrm{O4^{vi}}$	0.84 (3)	2.10 (3)	2.827 (3)	144 (3)
$\mathrm{N4-H4}C\cdots\mathrm{O1}$	0.89 (3)	2.13 (3)	2.996 (3)	163 (3)
$\mathrm{O6-H6\cdots O5^{v}}$	0.85	2.26	3.106 (3)	180
$\mathrm{C5-H5\cdots O2^{vii}}$	0.95 (3)	2.35 (3)	3.070 (3)	132 (2)

Symmetry codes: (i) $-x+\frac{1}{2}, y-\frac{1}{2}, -z+2$; (ii) $-x+\frac{1}{2}, y-\frac{1}{2}, -z+1$; (iii) $-x, y-1, -z+1$; (iv) $-x, y, -z+1$; (v) x, y, z; (vi) $-x, y, 2-z$; (vii) $\frac{1}{2}-x, \frac{1}{2}+y, 2-z$.

162.2 (2), χ^1 = N4—C5—C4—C3 61.4 (2), χ^2 = C5—C4—C3—C2 167.1 (2), χ^3 = C4—C3—C2—N3 175.6 (2), χ^4 = C3—C2—N3—C1 −105.4 (3), χ^{51} = C2—N3—C1—N1 −172.0 (3), χ^{52} = C2—N3—C1—N2 6.2 (4)°.

The crystal structure consists of alternate layers of L-arginine molecules and hydrogen selenite ions, stacked along the *c* axis and held together by hydrogen bonds, as shown in Fig. 4. This layer configuration is similar to that found in the crystal structure of LAP.

There is an extensive three-dimensional hydrogen-bonding network interconnecting the anions and the cations which is shown in Fig. 4. Full hydrogen-bond capability of the NH_2 and NH_3 groups is achieved in this structure, every H atom being donated to an O atom of either the carboxyl group of the cation or to one of the O atoms of the anion. The range of $\mathrm{H}\cdots A$ hydrogen-bond distances is 1.8 (4)–2.26 Å. Details of the hydrogen bonds are given in Table 3. Graph-set analysis (Bernstein *et al.*, 1995) shows that the hydrogen-bond network can be understood in terms of three groups of interactions: hydrogen bonds linking $HSeO_3^-$ ions, hydrogen bonds between $HSeO_3^-$ and L-ARG$^+$ ions and hydrogen bonds between L-ARG$^+$ ions. Below, the descriptors of the most important hydrogen-bonding patterns are given. The notation follows Grell *et al.* (1999): $C^a_d(p)$ = chain, $R^a_d(p)$ = ring, where *p* is the period of the pattern, the superscript denotes the number of hydrogen-bond acceptors and the subscript the number of hydrogen-bond donor H atoms. These two last parameters are omitted if equal to one. A descriptor is of the first level for the patterns containing only one type of hydrogen bond, those of the second-level arise from pairwise combinations of two distinct types of hydrogen bonds. The hydrogen selenite ions are linked in chains running along the *b* axis, for which the appropriate graph-set descriptor is *a*-*C*(4). $HSeO_3^-$–L-Arg$^+$ moieties are linked in chains, with second-level graph-descriptors *bi*-$C^2_2(13)$ and *de*-$C^1_2(4)$, where each hydrogen bond was labeled *a*–*j* following Table 3. H_2O–L-ARG$^+$ are linked in rings, with second-level graph descriptors *cj*-$R^2_4(15)$. The hydrogen bonds linking the arginine cations directly show distinct patterns. At the first level, the graph-set descriptors of these patterns are *c*-$C^2_2(10)$, *g*-*C*(5) and *h*-$R^2_2(10)$, while at the second level the patterns *cg*-$R^1_2(22)$, *ch*-$C^2_2(15)$ and *gh*-$R^4_2(15)$ are found.

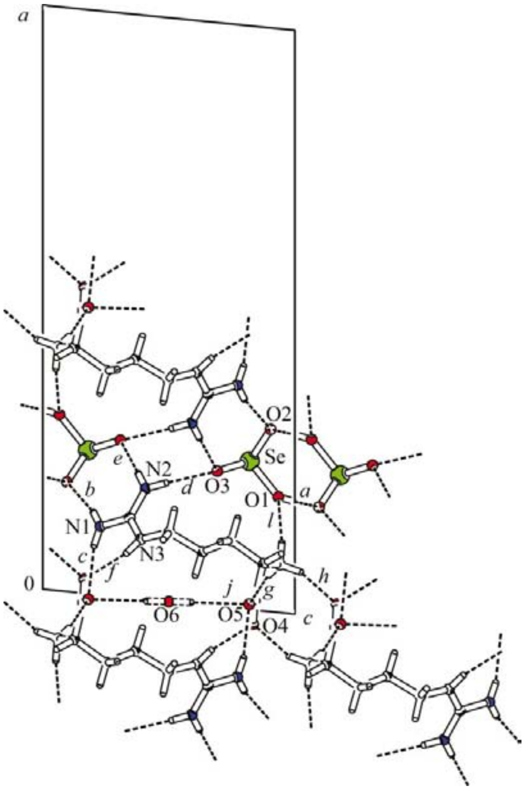

Figure 4
Packing diagram projected on the (010) plane showing the hydrogen-bonding scheme.

Low-temperature X-ray measurements on both powder and single crystals are underway to unravel the origin of the phase transition observed in the DSC measurements. Dielectric constant measurements are also underway and will be reported elsewhere.

This work was supported by FCT (Fundação para a Ciência e a Tecnologia).

References

Allen, F. H., Kennard, O., Watson, D. G., Brammer, L., Orpen, A. & Taylor, R. (1987). *J. Chem. Soc. Perkin. Trans. II*, pp. S1–S19.

Aoki, K., Nagano, K. & Iitika, Y. (1971). *Acta Cryst.* B**27**, 11–23.

Bernstein, J., Davis, R. E., Shimoni, L. & Chang, N.-L. (1995). *Angew. Chem. Int. Ed. Engl.* **34**, 1555–1573.

Eimerl, D., Velsko, S., Davis, L., Wang, F., Loiacona, G. & Kennedy, G. (1989). *IEEE J. Quantum Electron.* **QC-25**, 179–193.

Enraf–Nonius (1989). *CAD*-4 *Software*, Version 5.0. Enraf–Nonius, Delft, The Netherlands.

Grell, J., Bernstein, J. & Tinhofer, G. (1999). *Acta Cryst.* B**55**, 1030–1043.

IUPAC-IUB Commission on Biochemical Nomenclature (1975). *Biochem. J.* **149**, 1–16.

Johnson, C. K. (1976). *ORTEP*II. Report ORNL-5138. Oak Ridge National Laboratory, Tennesee, USA.

Kurtz, S. K. & Perry, T. T. (1968). *J. Appl. Phys.* **39**, 3798–3813.

Matos Gomes, E. de, Matos Beja, A., Paixão, J. A., Alte da Veiga, L., Ramos Silva, M., Martín-Gil, J. & Martín-Gil, F. J. (1995). *Z. Kristallogr.* **210**, 929–933.

Monaco, S. B., Davis, L. E., Velsko, S. P., Wang, F. T., Eimerl, D. & Zalkin, A. (1987). *J. Cryst. Growth*, **85**, 252–255.

Nardelli, M. (1999). *J. Appl. Cryst.* **32**, 563–571.

North, A. C. T., Phillips, D. C. & Mathews, F. S. (1968). *Acta Cryst.* A**24**, 351–359.

Paixão, J. A., Matos Beja, A., Ramos Silva, M., Matos Gomes, E. de, Martín-Gil, J. & Martín-Gil, F. J. (1997). *Acta Cryst.* C**53**, 1113–1115.

Sheldrick, G. M. (1997*a*). *SHELXL*97. University of Göttingen. Germany.

Sheldrick, G. M. (1997*b*). *SHELXS*97. University of Göttingen. Germany.

Spek, A. L. (1997). *HELENA*. University of Utrecht, The Netherlands.

Spek, A. L. (2001). *PLATON*. University of Utrecht, The Netherlands.

Yokotani, A., Sasaki, T., Yoshida, K. & Nakai, S. (1989). *Appl. Phys. Lett.* **55**, 2692–2693.